Available online www.jocpr.com

Journal of Chemical and Pharmaceutical Research, 2017, 9(2):85-91

Research Article

ISSN : 0975-7384
CODEN(USA) : JCPRC5

Binding Study of Thiamine Hydrochloride to Bovine Serum Albumin: Spectroscopic and Molecular Modeling Methods

Mallappa M[1], Shivakumar A[2], Babu Giriya Gowda[1]*, NageshBabu R[1] and Jyoti Sharma[2]

[1]Department of Chemistry, Maharani's Science College for Women, Bangalore, India
[2]Department of Agro informatics, Shobith University, Modipuram, Meeruth, Uttar Pradesh, India

---

ABSTRACT

The interaction between Vitamin B_1, thiamine hydrochloride (TAH), and bovine serum albumin (BSA) was studied by spectroscopic and computational methods. The native fluorescence of BSA was quenched by TAH. Stern-Volmer quenching constant was calculated at different temperatures which suggested a static mechanism. The association constant (K_a) was calculated from fluorescence quenching studies, which decreased with temperature rising. TAH competed well with warfarine for hydrophobic subdomain IIA (Sudlow's site I) on the protein. Enthalpy and entropy changes during the interaction of TAH with BSA were obtained using van't Hoff plot, which showed an entropy - driven process and involvement of hydrophobic forces ($\Delta H^o > 0$ and $\Delta S^o > 0$). Optimized docked model of BSA-TAH mixture confirmed the experimental results.

Keywords*:* Thiamine hydrochloride; Bovine serum albumin; Binding; Fluorescence; Molecular docking

---

INTRODUCTION

The vitamins are a disparate group of compounds; they have little in common either chemically or in their metabolic functions. Nutritionally, they form a cohesive group of organic compounds that are required in the diet in small amounts (micrograms or milligrams per day) for the maintenance of normal health and metabolic integrity [1]. Multivitamin pharmaceutical preparations containing mixtures of these substances are very interesting for analysis, and most of them include the water-soluble B-group. The term B-group vitamins usually refers to thiamine, riboflavin, pyridoxine, nicotinic acid, pantothenic acid, biotin, cyanocobalamine and folic acid [2]. Vitamins are reported to reduce the damage by free radicals and check degenerative disease [3]. The vitamin B_1 family consists of the pyrimidyl-substituted thiazole, thiamine, and its phosphate esters. The principal biologically active form of thiamine, TDP, is a coenzyme in several enzyme complexes that play vital roles in the metabolism of carbohydrates, fats, and alcohol [4]. Thiamine Hydrochloride (Figure 1) chemically is 3-[(4- amino-2-methylpyrimidin- 5-yl) methyl]-5-(2- hydroxyethyl)-4- methylthiazolium chloride hydrochloride, having molecular formula: $C_{12}H_{17}ClN_4OS$. HCl [5].

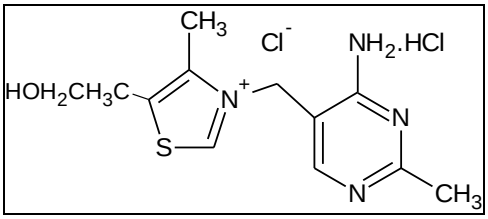

Figure 1: Thiamine Hydrochloride (Vitamin B_1)

Serum albumins are the major soluble protein constituents of the circulatory system, and include 50 - 60% of the total amount of plasma proteins [6]. They bind metabolites, endogenous molecules, hormones, drugs, and so on [7]. The most important property of this group of proteins is that they serve as transporters for a variety of compounds such as drugs, fatty acids, and so on [8]. Knowledge of interaction mechanism between drugs and plasma proteins is of crucial importance in the pharmacodynamics and pharmacokinetics of drugs [9,10].
Bovine serum albumin (BSA) is one of the most extensively studied of this group of proteins, particularly because of its structural homology with human serum albumin (HSA). BSA molecule is made up of three homologous domains (I, II, III) that are divided into nine loops (L1 - L9) by 17 disulfide bonds. Each domain in turn is the product of two subdomains (IA, IB, etc.). X-ray crystallographic data show that the albumin structure is predominantly α -helical, with the remaining polypeptide occurring in turns and in extended or flexible regions between subdomains [11]. In this work, interaction of TAH with BSA is investigated by spectroscopic and molecular modeling methods.

EXPERIMENTAL SECTION

Equipments and materials

BSA (>96%, essentially free from fatty acid, lyophilized powder) was purchased from Sigma (USA). BSA solution was prepared in sodium phosphate buffer (PBS, 0.1 M, pH 7.4) and was kept in the dark at 4ºC and used soon after preparation. TAH powder was obtained from Global Calcium (Hosur, India). All other chemicals were of analytical reagent grade and millipore water (resistivity of millipore water is 20 MΩ) was used throughout the experiment.

Fluorescence spectroscopy

Fluorescence emission spectra of BSA were recorded from 290 to 500 nm (λ_{ex} = 265 nm) on a Hitachi spectrofluorometer Model F- 2700 (Hitachi, Tokyo, Japan) with slit widths of 5 nm. A sample solution (2.0 mL) containing BSA (30.0 μM) and small aliquots of a stock solution (80.0 μM) of TAH was added into a 1cm quartz cuvette at intervals of 5 min.

Absorption spectroscopy

Absorption spectra were recorded on Ellico UV-visible spectrophotometer (India) using quartz cuvettes of 1 cm. The absorption spectra were recorded for free BSA and for its mixture with TAH.

Viscosity measurements

The viscosity measurements of protein (1.0×10^{-3} mol L^{-1}) in the presence and absence of TAH were made in a thermostatic water-bath at 25ºC. The data were presented as $(\eta/\eta_0)^{1/3}$ versus r [12], where η and η_0 are the viscosities of BSA in the presence and absence of TAH respectively. Viscosity values were calculated from the observed flow time of BSA containing solutions (t) and corrected for buffer solution (t_0), $\eta = (t - t_0)/t_0$.

Molecular docking study

For docking calculations, the crystal structure of BSA (PDB code 3V03) was downloaded from the protein data bank (PDB) (www.pdb.org). Atomic missed data of the protein was modeled by MODELLER version 9.10[12] using HSA (PDB code 1AO6) as a template. Atomic coordinates of TAH were built using Hyperchem program (version 8.0) in PDB format. The TAH structure built with this manner was geometrically optimized by Polak-Ribiere's conjugate gradient method implemented in Hyperchem program. The modeled protein was selected for docking process to study the interactions with TAH. The optimized structure of TAH was used as input of AutoDockTools (ADT) and the partial charges of atoms were calculated using Gasteiger–Marsili procedure. Using AutoGrid tools, the grid maps were generated adequately large to include regions of the BSA where, according to experimental data, estimated as binding sites.
In all cases, a grid of 46 x 74 x 56 points in the Cartesian space (x, y, z) and a grid spacing of 0.375 A^o was used. The most suitable structure for TAH was optimized by rotation of all single bonds in the molecule. The grid parameter and the docking parameter files were set up by the AutoDock Tools program. Population size was 256 and a maximum number of 2,500,000 were used for energy evaluations. Default settings were used for all other parameters. Docking calculations were carried out with the rigid BSA and flexible TAH using a Lamarckian genetic algorithm implemented in AutoDock version 4.2.3(13). The most suitable conformations of BSA-TAH complexes, in terms of energy and cluster population, were selected for molecular dynamics studies. Molecular graphics were prepared by VMD version 1.8.9 [13].

RESULTS AND DISCUSSION

Fluorescence quenching of BSA in the presence of TAH

Fluorescence spectrum of BSA contains a single peak with the maximum intensity at 340 nm (λ_{max}) as was shown in Figure 2. The emission is due to the three amino acids in BSA: tryptophan (Trp), tyrosine (Tyr), and phenylalanine (Phe) [14]. TAH did not emit at the near-UV and visible wavelengths. Incubation of BSA solution with different concentrations of TAH (final volumes of 2 mL) causes a gradual reduction in fluorescence intensity of the mixture. The fluorescence data were introduced to Stern-Volmer equation (Equation 2):

$$F_0/F = 1 + K_q\tau_0 [Q] = 1 + K_{SV} [Q] \quad (2)$$

where F_0 and F are the fluorescence intensities of BSA in the absence and presence of TAH. τ_0 is the average fluorescence lifetime of the biomolecule and equals to 10^{-8} s; K_q is the apparent bimolecular quenching rate constant. K_{SV} is the Stern – Volmer quenching constant and [Q] is the concentration of quencher (TAH).

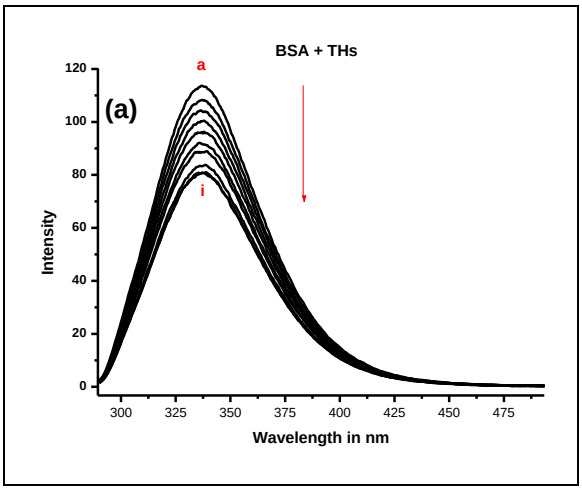

Figure 2: Fluorescence spectra of BSA in the presence of increasing amounts of TAH (pH = 7.4, *T* = 298 K, λ_{ex} = 265 nm). [TH] = 3.0 × 10^{-5} mol L^{-1} and [BSA] =01.8 × 10^{-4} mol L^{-1}

The plot of Stern – Volmer equation for BSA- TAH mixture at 25ºC is shown in Fig. 3A. Linear Stern – Volmer plot indicates a single quenching mechanism, either static (due to complex formation) or dynamic (due to collision). Moreover, as is shown in Table 1, K_{SV} decreases with rising temperature, which indicates that the fluorescence quenching of BSA is static (in the case of dynamic quenching, an increase in K_{SV} is observed with rising temperature) [15].

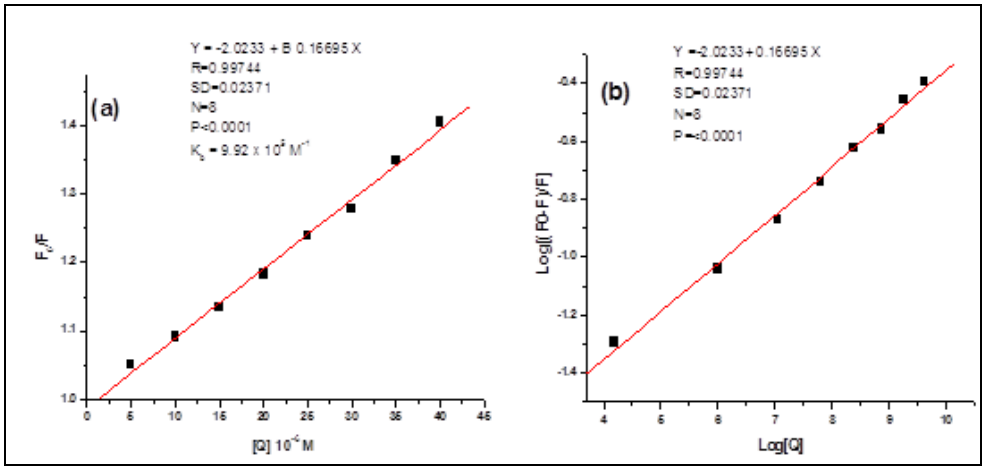

Figure 3 (A): Stern-Volmer plot of quenching of BSA by TAH (Q) at 25ºC. (B) Plot of log [(*F*$_0$-*F*)/*F*] *versus* log [Q]. pH = 7.4, λ_{ex} = 265 nm,λ_{em} = 340 nm). [TAH] = 3.0 × 10^{-5} mol L^{-1}

Table 1: Stern-Volmer quenching constant K_{SV} and K_q values

System	Temperature (T)	K_{SV} (x 10^4) (L/mol)	K_q (x10^{13}) (L/mol s)
BSA - TAH	288	6.32 ± 0.07	9.92 ± 0.12
	298	5.91 ± 0.03	8.37 ± 0.05
	308	3.53 ± 0.05	5.64 ± 0.03

Binding constant and binding sites

The association constant (K_a) of BSA-TAH complex and the number of equivalent binding sites on macromolecule (n) can be calculated by using Eq. 3, using the fluorescence quenching data of Fig. 3B.

$$\log [(F_0 - F)/F] = \log K_a + n \log [Q] \quad (3)$$

The calculated K_a and n values at different temperatures are presented in Table 2. Decreasing association constant with temperature shows an endothermic interaction (positive enthalpy change during complex formation). The values of n at the experimental temperatures were approximately equal to 1, which indicated that there was one class of binding site to TAH with BSA. In BSA, the tryptophan residues involved in binding can be either Trp134 or Trp212 of both tryptophans in BSA, and Trp134 is more exposed to a hydrophilic environment, whereas Trp212 is deeply buried in the hydrophobic loop [16]. Therefore, from the value of n, it was proposed that TAH most likely bind to the hydrophobic pocket located in subdomain IIA. That is to say, Trp212 is near or within the binding site [17].

Table 2: Thermodynamic parameters of TAH-BSA system

System	Temp (K)	Binding constant (L/molx10^3)	No. of binding sites (*n*)	ΔH^o (k J/mol)	ΔS^o (J/Kmol)	ΔG^o (kJ/mol)
BSA-TAH	288	6.32 ± 0.44	0.937	26.16	160.54	-21.68
	298	4.07± 0.21	0.917			
	308	2.81± 0.25	0.911			

Binding mode

Fluorescence spectroscopy is widely used in studying the kinds of forces acting in the interaction between a biosystem and drug molecules [15,18,19]. Therefore, the changes in enthalpy and entropy during the process (ΔH^o and ΔS^o) were calculated according to van't Hoff equation:

$$ln\ \text{Ka} = -\Delta H^o/\text{RT} + \Delta S^o/\text{R} \quad (4)$$

Figure 4 represents a good linear relationship between *ln* Ka and 1/T, which means that ΔH^o is constant in the range of temperatures discussed. The values of ΔH^o and ΔS^o could be calculated from the slope and intercept of the van't Hoff plot, respectively. As is shown in Table 2, both ΔH^o and ΔS^o are positive, which shows that hydrophobic forces are the main acting forces in TAH-BSA interaction according to Ross and Subramanian [19].

The Gibbs free energy change (ΔG^o) can be calculated using Eq. 5:

$$\Delta G^o = \Delta H^o - \text{T}\Delta S^o = -\text{RT}\ ln\text{Ka} \quad (5)$$

The negative value of ΔG^o (-21.68 kJ mol^{-1}) shows the spontaneity of the entropy – driven interaction ($\Delta S^o > 0$, $\Delta H^o > 0$) between TAH and BSA.

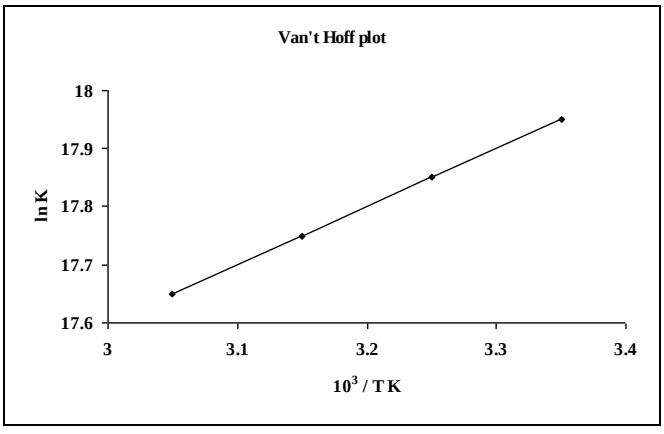

Figure 4: Van't Hoff plot of ln *K* vs. 1/T for TAH-BSA system

Binding distance

Fluorescence resonance energy transfer (FRET) [20] occurs whenever the emission spectrum of the fluorophore (donor) overlaps with the absorption spectrum of the acceptor. Basically, efficiency of the FRET mainly

depends on following three parameters (i) the distance between donor and acceptor (which must be within the specified Förster distance of 2 to 8 nm); (ii) appreciable overlap between the donor fluorescence and acceptor absorption band and (iii) proper orientation of the transition dipole of the donor and acceptor. The distance between the donor and acceptor could be calculated according to Förster's theory [21]. The efficiency of energy transfer, E, was calculated using the equation (6):

$$1 - \frac{F}{F_0} = \frac{R^6_0}{R^6_0 + r^6} \text{ ---------- (6)}$$

where E is the efficiency of energy transfer, F and F_0 are the fluorescence intensities of donor in the presence and absence of the acceptor, respectively. r represents the acceptor-donor distance and R_0 is the critical distance when the transfer efficiency is 50 %. R_0 can be expressed as

$$R^6_0 = 8.8 \times 10^{-25}\, k^2 N^{-4} \Phi J \text{ ---------- (7)}$$

where k^2 is the spatial orientation factor of the dipole, N is the refractive index of the medium, Φ is the fluorescence quantum yield of the donor and J is the overlap integral of the fluorescence emission spectrum of the donor and the absorption spectrum of the acceptor(22). J is given by Eq.(8)

$$J = \frac{\Sigma F(\lambda)\, \varepsilon(\lambda)\, \lambda^4\, \Delta\lambda}{\Sigma F(\lambda)\, \Delta\lambda} \text{ ------- (8)}$$

where F(λ) is the fluorescence intensity of the fluorescent donor at wavelength λ, ε(λ) is the molar absorption coefficient of the acceptor at wavelength λ. In the present case, $k^2 = 2/3$, n = 0.93 and Φ = 0.16 [22,23]. From Equations (6) − (8), J = 1.875×10^{-14} (cm^3 L/mol), Ro = 2.851 nm, E = 0.076 and r = 4.97 nm each other and hence they have strong binding between them [24]. Further, the observed donor-to-acceptor distance r < 8 nm revealed the presence of static quenching in the interaction [25].

UV-Vis absorption study

UV-vis absorption spectroscopy is a very simple method and can be used to explore the complex formation. Figure 4 shows UV - vis absorption spectra of BSA in the absence and presence of TAH. BSA has two absorption peaks; the absorption peak at ~208 nm reflects the framework conformation of the protein [26], and the peak at ~279 nm appears to be due to the aromatic amino acids (Trp, Tyr, and Phe) [27]. On gradual addition of TAH to BSA solution, the intensity of the peak at 279 nm increases, which means the change in the environment around the mentioned amino acids. The drug (as is obvious from its structure in Figure 1) did not absorb at this wavelength range.

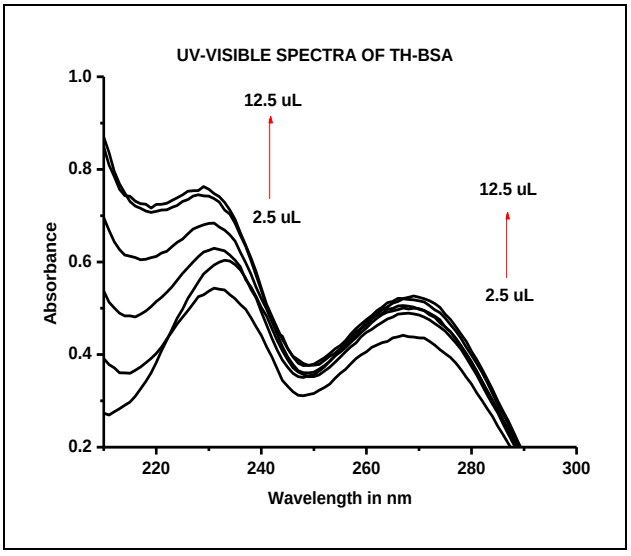

Figure 4: Absorption spectra of TAH in the absence and presence of increasing amounts of BSA, [TAH] = 8.0×10^{-5} mol L^{-1}, [BSA] = 0.0-12.5×10^{-5} mol L^{-1}. (*T* = 25 °C)

Viscosity measurements

Viscosity measurement is an effective tool to study the binding mode of small molecules to BSA. A classical intercalation binding demands the space adjacent base pairs to be large enough to accommodate the bound ligand and elongate the double helix, resulting in an increase of BSA viscosity. A non-classical intercalation or a

groove mode would reduce the BSA viscosity [28]. The viscosity measurements were taken by varying the concentration ratio of BSA and TAH. The values of relative specific viscosity $(\eta/\eta_0)^{1/3}$ vs. [TAH] / [BSA] were plotted in the absence and presence of BSA as shown in Figure 5.

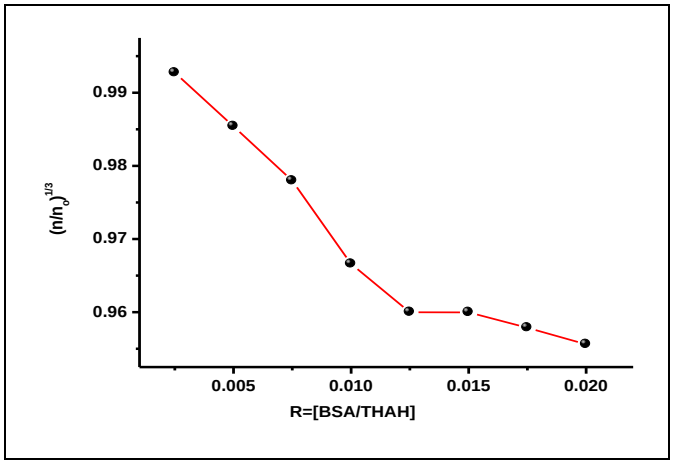

Figure 5: Effect of increasing concentration of TAH on the relative viscosity of BSA

As shown in figure, the relative specific viscosities of BSA depends on the concentration of TAH, which increases with the value of [TAH]/[BSA]. This indicates a non-classical intercalation mode of binding possibly a groove binding *via* hydrophobic interaction between TAH and BSA.

Molecular docking analysis

Molecular docking technique is an attractive scaffold for mechanistic studies. The study is performed by placing a small molecule into the binding site of the target- specific region of the protein, mainly in a non-covalent fashion. The docked model of BSA-TAH mixture was shown in Figure 6 (A), in which TAH is surrounded by hydrophobic side chains of amino acids such as Ile-202, Leu-213, Val-240, Lys-242, etc. The model confirms the predominance of hydrophobic interactions in the BSA-TAH complex. Moreover, two hydrogen bonds between hydrogen atoms of TAH and the adjacent oxygen atoms of Glu-243 (1.7 A) and Glu-251 (1.9 Aº) were found [Figure 6 (B)], considering the distance between donor and acceptor atoms [29]. Hydrogen bonding decreases the polarity of TAH, and increased tendency for hydrophobic interactions is the result.

The association constant (K_a) and free energy change (ΔG^o) for the binding of TAH to BSA were calculated at 25ºC according to the docked model as 1.21 x 10^4 M^{-1} and -6.6 kcal mol^{-1}, respectively. The results closely matched the experimental data.

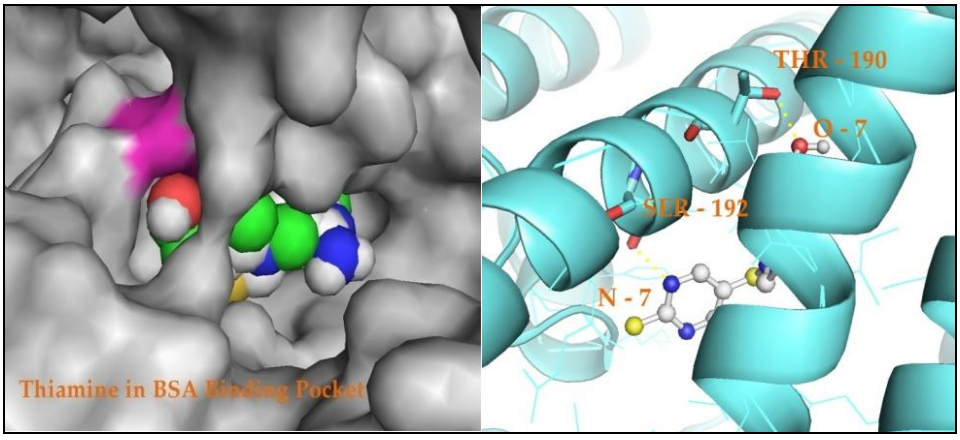

Figure 6: (A) Molecular docked model of TAH (sphere representation) located within the hydrophobic pocket of BSA. (B) The hydrogen bond interaction (Red dotted line) between TAH (stick) and BSA (cartoon)

CONCLUSIONS

The interaction between thiamine hydrochloride, and BSA was studied by spectroscopic and molecular docking methods. Quenching of the native fluorescence of BSA was observed in the presence of the drug. Moreover,

TAH has a hyperchromic effect on BSA absorption centered at 279 nm. The results of synchronous fluorescence studies showed that TAH interacts mainly with Tyr-rich subdomains of BSA. The predominance of hydrophobic interactions was concluded from both experimental results and molecular docking model. Optimized docked structure of BSA-TAH with minimum energy showed that TAH is surrounded by hydrophobic amino acid residues. Theoretical calculations also revealed the formation of two hydrogen bonds between TAH and glutamic acid residues which led to increased hydrophobicity of the drug. Closely matched values for thermodynamic parameters (association constant and Gibbs free energy) were obtained from fluorescence quenching measurements on one hand, and molecular docking calculations on the other hand.

ACKNOWLEDGMENT

Financial support (F.No. 42-308/2013 (SR)) from University Grants Commission, New Delhi, India is gratefully acknowledged. Thanks are also due to Dr. Siddalingeshwar, Department of Physics, MSRIT, Bangalore for providing spectrofluorimetric instrumental facilities.

REFERENCES

[1] P Ortega; ML Barrales; DC Fernandes; DA Molina. *Anal Chem*. **1998**, 70, 271.
[2] RA Jacab; G Sotoudeh. *Nutri Clin Care.* **2002**, 5, 66-74.
[3] PL Lynch; IS Young. *J Chromatography*. **2000**. 881, 267-84.
[4] P Moreno; V Salvado. *J. Chromatography A*. **2000**. 870, 207-215.
[5] B Zhao; SY Tham; J Lu; MH Lai; LKH Lee; SM Moochhala. *J Pharm Pharm Sci*. **2004**. 7(2), 200-204.
[6] DC Carter; JX Ho. *Adv. Protein Chem*. **1994**, 45, 153-203.
[7] MS Highley; EA DeBruijin. *Pharm Res*. **1996**, 13, 186-195.
[8] D Shcharbin; M Janicka; M Wasiak; B Palecz; M Przybyszewska; M Zaborski; M Bryszewska. *Biochim Biophys.Acta*. **2007**, 1774, 946-951.
[9] J Jayabharathi; K Jayamoorthy; V Thanikachalam; R Sathishkumar. *Spectrochim. Acta A.* **2013**, 108, 146-150.
[10] N Shahabadi; FS Moradi. *Spectrochim. Acta A*, **2014**, 118, 422-429.
[11] T Peters; All About Albumin. Biochemistry, Genetics and Medical Applications; Academic Press: San Diego **1996**.
[12] A Sali; TL Blundell; *J Mol Biol*. **1993**, 234, 779-815.
[13] GM Morris; DS Goodsell; RS Halliday, R Huey, Hart WE, RK Belew, AJ Olson. *J Comput Chem.* **1998**, 19, 1639-1662.
[14] P Qin; R Liu; X Pan; X Fang, Y Mou. *J Agric Food Chem*. **2010**, 58, 5561-5567.
[15] Y Zhang; X Xiang; P Mei; J Dai; L Zhang; Y Liu. *Spectrochim Acta A*. **2009**, 72, 907-914.
[16] D Subbaih; AK Mishra. *J Pharm Biome Anal.* **2005**, 38, 556-563.
[17] Z Cheng; Y Zhang. *J Mol Struct.* **2008**, 889, 20-27.
[18] Y Hu; Y Liu; J Wang; X Xiao; S Qu. *J Pharm Biomed.* **2004**, 36, 915-919.
[19] PD Ross, S Subramanian. *Biochem*. **1981**, 20, 3096-3102.
[20] JR Lakowicz. Principles of fluorescence spectroscopy, Plenum, New York, **2006**, 281-283.
[21] T Förster; O Sinanoglu. Modern quantum chemistry, Academic Press: New York, USA, **1966**, 93-136.
[22] S Bi; D Song; Y Tian. *Spectrochim Acta A*, **2005**, 61, 629-636.
[23] FL Cui; J Fan; DL Ma. *Anal Lett*. **2003**, 36, 2151-2166.
[24] CQ Jiang; MX Gao; XZ Meng. *Spectrochim. Acta. A*. **2003**, 59, 1605-1610.
[25] FL Cui; J Fan; JP Li. *Bioorg Med Chem*. **2004**, 12, 151-157.
[26] Q Yang; J Liang; H Han. *J Phys Chem B*. **2009,** 113, 10454-10458.
[27] F Wang; W Huang; ZX Dai. J Mol Struct. **2008**, 875, 509-514.
[28] Hao-Yu Shen, Xiao-Li Shao, Hua Xu, Jia LI, Sheng-Dong. Pan. *Int J Electrochem Sci*. **2011**, 6, 532-547.
[29] M Karplus; JA McCammon. *Nat Struct Biol*. **2002**, 9, 646-652.